

## Kurze Mitteilungen

Bis am 15. des Monats bei der Redaktion eingehende Kurze Mitteilungen werden in der Regel am 15. des folgenden Monats veröffentlicht. Es werden auch Manuskripte aus dem Ausland angenommen. Maximalumfang: 6 Schreibmaschinenseiten (alles inbegriffen)

### Oxidative Cleavage of Aromatic Azines with Periodic Acid; MO Model for the Reaction Intermediate\*

#### Summary

Cleavage of benzalazine (and other azines) with periodic acid may initially involve, as a single step, the addition of  $\text{IO}_4^-$  (or its hydrate) across the conjugated azine system, to give an iodate I(V) complex; this view is supported from MO symmetry rules.

It was recently shown<sup>1</sup> that aromatic or heterocyclic azines when treated with periodic acid at room temperature caused brisk evolution of nitrogen; extraction of the reaction mixture gave the parent aldehyde (or ketone) in over 95 per cent yield, indicating that the oxidative cleavage was complete.

The formation of nitrogen may arise through collapse of an association complex initially formed between periodate anion and a resonance structure of the azine, for example, benzalazine (1,4-diphenyl-2,3-diazabuta-1,3-diene). The structure of the complex and the pathway of formation of nitrogen are shown in Fig. 1.<sup>1</sup>

Examination of the association complex (Fig. 1) showed that the azine had already suffered a two-electron oxidation (formation of two bonds), and the question was whether to depict a transition complex with iodine(VII) or with iodine(V). Our statement<sup>1</sup> that the formation of a complex (Fig. 1) is a symmetry-allowed reaction, as predicted from MO symmetry rules, was based on the assumption that iodate ion I(V) should be depicted. However, the e. s. r. evidence<sup>1</sup> regarding the action of both oxidants ( $\text{H}_5\text{IO}_6$  and  $\text{HIO}_3$ ) on azines, particularly a low-field peak at 1.864 kG due to a binuclear, triplet-state species that is observed only for periodic acid, made it difficult to conceive the existence of a dimer species

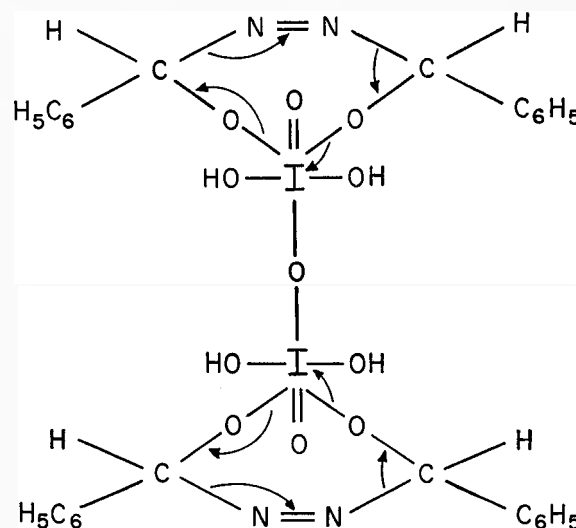
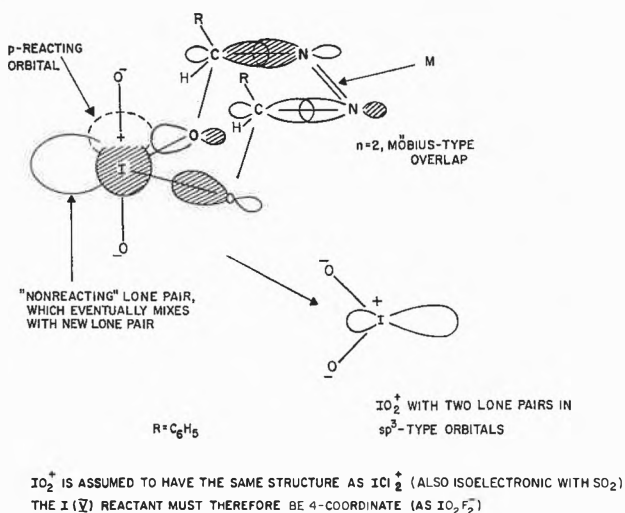


Fig. 1. Proposed structure of the association complex between periodate anion and a resonance structure of benzalazine

for the iodic acid (or its ion) in solution. Moreover, the ability of an anion of periodic acid (but not iodic acid) to dimerize in aqueous solution has been reported<sup>2</sup> and confirmed by the laser-Raman spectra.<sup>1</sup> Consequently, the formation of such a complex may involve, as a *single step*, the addition of  $\text{IO}_4^-$  (or its hydrate) across the

\* Received November 30, 1971. Part IX of the series, Periodic acid, a novel oxidant. Part VIII: A. J. FATIADI and R. SCHAFFER, *Experientia* 27 (1971) 1139.



Scheme 1

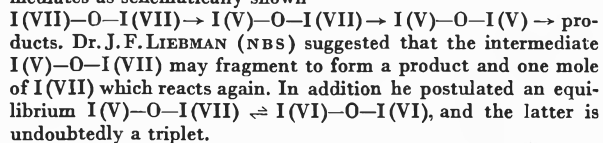
conjugated azine system to give an iodate I (V) complex\*; this view is in agreement with that of another worker.<sup>3</sup> This view is also in agreement with ZIMMERMAN'S<sup>4</sup> simplified MO approach to predict a transition state of the chemical reaction, and as a result of selection rules for electrocyclic reactions, the course of chemical reactions, including oxidation reactions of organic substrates, can now be predicted.<sup>5</sup> Also MO approach predicted the aromatic transition states for the DIELS-ALDER reaction<sup>6</sup> and more recently<sup>7</sup> this approach was extended to show the correlation between the orbital topology and geometry of molecules in the transition state for cyclic reactions, such as the WAGNER-MEERWEIN rearrangement, the 1,2-hydride shift, the allylic shift, and others.\*\*

Chemical reactions consist of the breaking of certain bonds between atoms and making of new bonds. In other words, in a chemical reaction certain orbitals must be vacated of electrons and others must be filled to create the new bonding situation.<sup>8</sup>

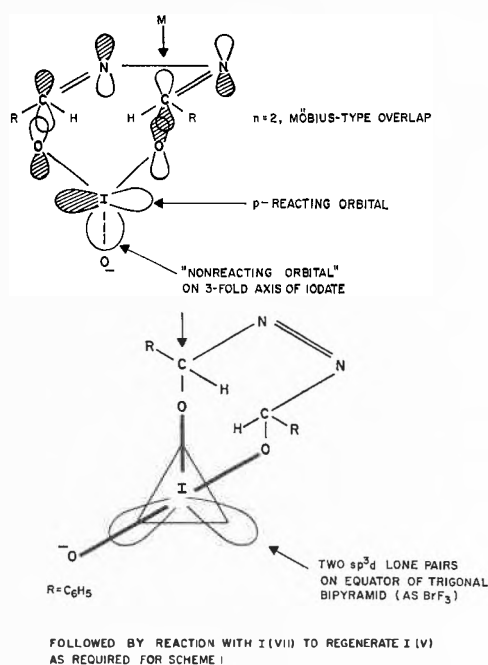
The molecular-orbital overlap in the transition state, particularly in the formation of the complex (Fig. 1) can be treated either by symmetry rules of WOODWARD and HOFFMAN<sup>9</sup> or by a topological approach of ZIMMERMAN.<sup>4</sup>

The ZIMMERMAN method<sup>4</sup> requires the classification of the transition state as either "Hückel-like", in which all overlapping pairs of reacting orbitals are bonded, or "Möbius-like", in which one, or an odd number of, anti-state bonding overlap(s) must occur. In a HÜCKEL

\* Formation of the association complex (Fig. 1) may involve intermediates as schematically shown



\*\* See, for example, on electrocyclic cycloaddition reactions [E. C. W. SCHEUNEMANN and W. G. LAIDLAW, *J. Amer. Chem. Soc.* 93 (1971) 5731] or on sigmatropic rearrangement of organometallic compounds with carbon-metal  $\sigma$  bonds [CHAN-CHEN SU, *ibid.* 93 (1971) 5655].



Scheme 2

transition state,  $4n + 2$  electrons form a closed shell (giving it stability), whereas  $4n$  electrons are required for stable, closed shells in a MÖBIUS state. It will be noted that  $4n$  electrons are involved in the azine oxidation with periodic acid (Fig. 1). Thus an "allowed" reaction may have either a HÜCKEL or MÖBIUS type of transition state, provided that the correct number of electrons is available to stabilize that transition state,<sup>5</sup> and provided that such an appropriate transition state may be formed.

When a transition metal complex is an oxidant [e.g.  $\text{CrO}_3$ ,  $\text{KMnO}_4$  or  $\text{Pb}(\text{OAc})_4$ ], the electrons enter the  $d$ -shell, so the reacting orbital must be the  $d$ -orbital they enter. It is necessary to classify this as either locally symmetric ( $\sigma$ -type) or antisymmetric ( $\pi$ -type) in order to know whether the transition state is of MÖBIUS or HÜCKEL type.<sup>5</sup> Unlike the transition metal oxidants, mentioned above, when iodine (VII) (periodate) is reduced to iodine (V) (iodate), here there are no vacant low-level  $d$ -orbitals to accommodate the electrons. Instead they behave as a "lone-pair"<sup>10</sup> occupying an orbital,

<sup>1</sup> A. J. FATIADI, *Chem. Ind. (London)* 1970, 64.

<sup>2</sup> G. J. BUIST and J. D. LEWIS, *Chem. Comm.* 1965, 66.

<sup>3</sup> J. S. LITTLER, University of Bristol (England), personal communication.

<sup>4</sup> H. E. ZIMMERMAN, *Angew. Chem. (internat. Ed.)* 8 (1969) 1.

<sup>5</sup> J. S. LITTLER, *Tetrahedron* 27 (1971) 81.

<sup>6</sup> M. J. S. DEWAR, *The Molecular Orbital Theory of Organic Chemistry*, McGraw-Hill, New York 1969.

<sup>7</sup> C. W. JEFFORD and U. BURGER, *Chimia* 25 (1971) 297.

<sup>8</sup> R. G. PEARSON, *Accounts Chem. Res.* 4 (1971) 152.

<sup>9</sup> R. B. WOODWARD and R. HOFFMAN, *Angew. Chem. (internat. Ed.)* 8 (1969) 781; R. HOFFMAN and R. B. WOODWARD, *Science* 167 (1970) 825; also: R. B. WOODWARD and R. HOFFMAN, *The Conservation of Orbital Symmetry*, Academic Press, New York 1970.

<sup>10</sup> F. A. COTTON and G. WILKINSON, *Advanced Inorganic Chem.*, 2nd Edition, Interscience, London 1966, p. 400, 571.

with  $\sigma$  character which will also be locally symmetric and which is directed along the three-fold axis of the  $\text{IO}_3^-$  pyramid.<sup>5</sup> One possible way for an "allowed" reaction between periodate and benzalazine should include an allowed decomposition of the iodine (V) analog of the complex (Fig. 1) as depicted in Scheme 1.

The intermediate produced by such reaction would be the tetracoordinated iodate complex, and this would be expected to have a structure like that of  $\text{IO}_2\text{F}_2^-$ , in which the lone pair occupies an equatorial position of a trigonal bipyramid. The structures of known halogen (III) compounds such as  $\text{ICl}_2^+$ ,  $\text{BrF}_3$  or  $\text{IF}_4^-$  suggest that lone pair orbitals may have some  $p$  character<sup>11</sup> which would permit an allowed decomposition of the iodate (V) analog of the complex (Fig. 1). This would also accord with the non-existence of a malaprade-type glycol fission by iodate.<sup>3, 5</sup>

The immediate difficulty, however, of imagining an additional step involving iodate ion I(V) to benzalazine to give the complex (Fig. 1) can be overcome by the possible pathway shown in Scheme 2. Note that some asymmetric mechanism must be active, since the oxygen atoms of  $\text{IO}_3^-$  are originally related by a three-fold axis which is lost in the product.

Thus an overall reaction between benzalazine and periodic acid is likely a two-step process involving an intermediate product.

The author thanks Dr. J.S. LITTLER, University of Bristol (England) for a stimulating discussion and a useful suggestion.

ALEXANDER J. FATIADI

Analytical Chemistry Division, Institute for Materials Research, National Bureau of Standards, Washington (D. C.) 20 234 (U. S. A.)

<sup>11</sup> E. JØRGENSEN, in *Halogen Chemistry*, Edition GUTMANN, Academic Press, New York 1967, p. 366, 369.

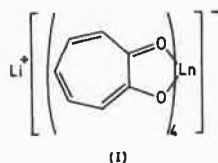
## Infrared Spectra of Tetrakis(tropolonato) Lanthanide(III) Chelates: Evidence for Crystal Field Effects\*

### Summary

The infrared spectra of the fourteen complex ions  $[\text{LnT}_4]^-$  ( $\text{Ln} = \text{La, Ce, Pr, Nd, Sm, Eu, Gd, Tb, Dy, Ho, Er, Tm, Yb, Lu}$ ;  $\text{T} = \text{tropolonato anion}$ ) have been determined. One band within the range  $480$  to  $510 \text{ cm}^{-1}$  is found to be significantly metal-sensitive and is accordingly assigned to the metal-oxygen stretching frequency,  $\nu \text{Ln-O}$ . This assignment is supported by comparison with the spectra of  $[\text{CuT}_2]$  and  $[\text{ScT}_3]$ .  $\nu \text{Ln-O}$  exhibits the double-humped relationship with  $4f$ -orbital population (with minima at  $4f^0, 4f^7$  and  $4f^{14}$ ) which is expected in the presence of crystal field stabilization.

It is now well established<sup>1-4</sup> that the variation in metal-ligand stretching frequency ( $\nu \text{M-L}$ ) through a series of isostructural  $3d$  transition metal complexes with identical ligand composition may be interpreted in terms of crystal field theory. This communication represents the first reported evidence from infrared spectra for the presence of crystal field stabilization in isostructural complexes of the  $4f^n$  lanthanide ions.

By contrast with the complexes of  $3d$  metal ions, those of the  $4f$  series generally crystallize with different numbers of coordinated solvent molecules so that an isostructural series is not usually realized. This difficulty is avoided in the tetrakis(tropolonato) complexes (I) which, in view of their identical 8-coordinate stoichiometry,<sup>5</sup> were chosen for the present study.



\* Received Dezember 2, 1971.

That the infrared spectra of the  $[\text{LnT}_4]^-$  complex ions exhibit identical band patterns (Fig. 1) is in support of their isostructural character. The band within the range  $490$  to  $520 \text{ cm}^{-1}$  exhibits the maximum sensitivity to the coordinated  $\text{Ln}$  (III) ion and, on this basis, is assigned to the vibrationally purest (least-coupled) metal-oxygen stretching frequency,  $\nu \text{Ln-O}$  (Table I).

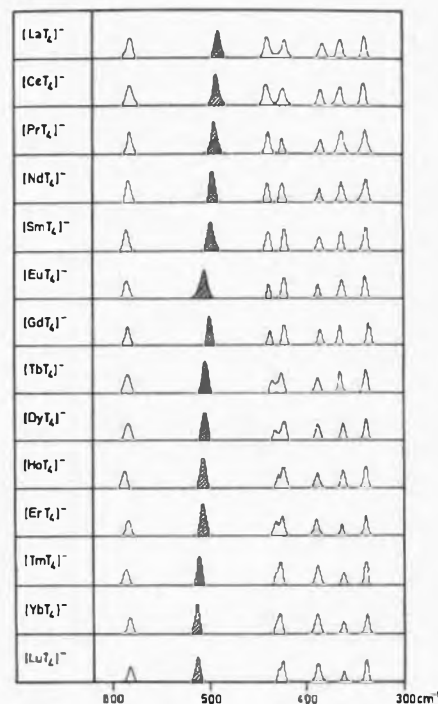


Fig. 1. Infrared spectra of complexes  $\text{Li}[\text{LnT}_4]$

Table I.  $Ln-O$  stretching frequencies ( $\nu Ln-O$ ) and ( $\nu-\nu_0$ ) values for  $Li [LnT_4]$  complexes

Complex	Ion configuration	$\nu Ln-O$ ( $cm^{-1}$ )	( $\nu-\nu_0$ ) ( $cm^{-1}$ )
Li [LaT <sub>4</sub> ]	4f <sup>0</sup>	490.5	0
Li [CeT <sub>4</sub> ]	4f <sup>1</sup>	492	0
Li [PrT <sub>4</sub> ]	4f <sup>2</sup>	494.5	1.0
Li [NdT <sub>4</sub> ]	4f <sup>3</sup>	496	1.0
Li [SmT <sub>4</sub> ]	4f <sup>5</sup>	499	2.0
Li [EuT <sub>4</sub> ]	4f <sup>6</sup>	502	3.0
Li [GdT <sub>4</sub> ]	4f <sup>7</sup>	500	0
Li [TbT <sub>4</sub> ]	4f <sup>8</sup>	504	2.0
Li [DyT <sub>4</sub> ]	4f <sup>9</sup>	505.5	2.0
Li [HoT <sub>4</sub> ]	4f <sup>10</sup>	506.5	1.0
Li [ErT <sub>4</sub> ]	4f <sup>11</sup>	508.5	1.5
Li [TmT <sub>4</sub> ]	4f <sup>12</sup>	510.5	1.5
Li [YbT <sub>4</sub> ]	4f <sup>13</sup>	512.5	1.5
Li [LuT <sub>4</sub> ]	4f <sup>14</sup>	512.5	0

Evidence in support of this assignment arises from a comparison of the spectra of  $[CuT_2]$ ,  $[ScT_3]$  and  $[LnT_4]^-$ . In  $[CuT_2]$ , the vibrationally purest  $\nu Cu-O$  band is at  $639\text{ cm}^{-1}$  since this band exhibits<sup>6</sup> the maximum shift towards lower frequency on <sup>18</sup>O-labelling. The corresponding vibration in  $[ScT_3]$ ,  $\nu Sc-O$ , has been assigned<sup>3</sup> to the band at  $583\text{ cm}^{-1}$  on the basis that this band exhibits the maximum shift on substitution of Sc(III) by other 3d transition metal(III) ions and because the shift parallels that of the crystal field stabilization energies (CFSE's), viz.  $Sc < Ti < V < Cr > Mn > Fe < Co > Ga$ . The values of  $\nu M-O$  for the complexes  $[CuT_2]$ ,  $[ScT_3]$  and  $[LnT_4]^-$  are in the order  $Cu > Sc > Ln$  which is the order expected if we consider that the bonding capacity of the metal ion in these three complexes is distributed over 4, 6 and 8 bonds, respectively.

YATSIMIRSKII and KOSTROMINA<sup>7</sup> have analysed the crystal field effects in complexes of 4f<sup>n</sup> ions. The variation of CFSE with 4f-orbital population has the double-humped shape which also characterizes the variation of CFSE in complexes of 3d<sup>n</sup> ions. Minima occur at the 4f<sup>0</sup>, 4f<sup>7</sup> and 4f<sup>14</sup> configurations, corresponding to those complexes which are not stabilized by the crystal field. Similar double-humped curves have been obtained<sup>8,9</sup> for the logarithms of the cumulative stability constants,  $\log \beta_n$ , and other thermodynamic parameters of various rare earth complexes. The variation of  $\nu Ln-O$  for the  $[LnT_4]^-$  complex ions is seen (Fig. 2) to follow a similar relationship.

Following the procedure previously employed<sup>1-4</sup> to interpret the variation of  $\nu M-L$  with 3d-orbital population in terms of crystal field theory, the  $\nu Ln-O$  values are considered to be comprised of contributions from three predominant effects. Firstly, the increase in mass of the coordinated ion through the 4f series will tend to decrease  $\nu Ln-O$ ; this effect will be small in view of the similar masses of the Ln(III) ions. Secondly, the lanthanide contraction will stabilize the Ln-O bonds with increasing 4f orbital population and this will lead to a substantial increase in  $\nu Ln-O$ . The third contribution

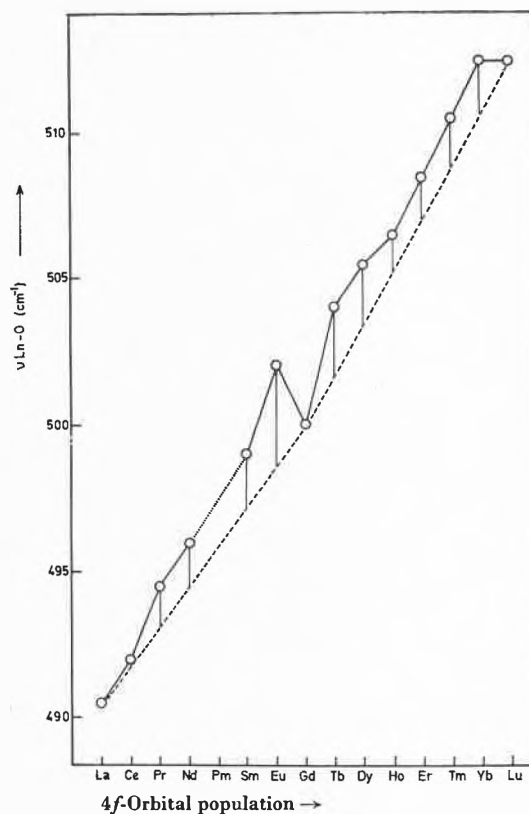


Fig. 2. Relationship between  $\nu Ln-O$  and 4f-orbital population for  $[LnT_4]^-$ . The lower dashed line is the interpolation line representing  $\nu_0$ . The vertical lines represent ( $\nu-\nu_0$ )

arises from the crystal field stabilization and this effect is absent from the complexes of La(III), Gd(III) and Lu(III) with 4f<sup>0</sup>, 4f<sup>7</sup> and 4f<sup>14</sup> configurations. Hence an interpolation line drawn through the points for 4f<sup>0</sup>, 4f<sup>7</sup> and 4f<sup>14</sup> in Fig. 2 is considered to represent the frequencies ( $\nu_0$ ) which would be realized in the absence of crystal field stabilization, i.e. those which arise from the resultant of the mass effect and the effect of the ionic contraction. The substantial positive slope of the interpolation line is in accordance with the considerable stabilization of the Ln-O bonds which is expected to accompany the contraction of the Ln(III) ions through the series.

<sup>1</sup> R. D. HANCOCK and D. A. THORNTON, *J. Mol. Structure* 4 (1969) 361; 6 (1970) 441.

<sup>2</sup> J. M. HAIGH, R. D. HANCOCK, L. G. HULETT and D. A. THORNTON, *J. Mol. Structure* 4 (1969) 369.

<sup>3</sup> L. G. HULETT and D. A. THORNTON, *Spectrochim. Acta* 27A (1971) 2089.

<sup>4</sup> G. S. SHEPARD and D. A. THORNTON, *Helv. Chim. Acta* 54 (1971) 2212.

<sup>5</sup> E. L. MUETTERTIES and C. M. WRIGHT, *J. Amer. Chem. Soc.* 87 (1965) 4706.

<sup>6</sup> H. JUNGE, *Spectrochim. Acta* 24A (1967) 1957.

<sup>7</sup> K. B. YATSIMIRSKII and N. A. KOSTROMINA, *Zhur. Neorg. Khim.* 9 (1964) 1793.

<sup>8</sup> D. L. CAMPBELL and T. MOELLER, *J. Inorg. Nucl. Chem.* 31 (1969) 1077.

<sup>9</sup> L. A. K. STAVELEY, D. R. MARKHAM and M. R. JONES, *J. Inorg. Nucl. Chem.* 30 (1968) 231.

On the basis of the above discussion, the difference ( $\nu-\nu_0$ ) between the observed and interpolated frequencies represents the contribution to  $\nu Ln-O$  arising from the crystal field stabilization. An analysis<sup>9</sup> of thermodynamic parameters for the lanthanide diglycollate and dipicolinate complexes reveals that crystal field effects operate for the lanthanide ions on a scale between one and two factors of ten smaller than the effects for the 3d transition metal ions. The mean value of ( $\nu-\nu_0$ ) for the  $[LnT_4]^-$  complexes is approximately one-twentieth of the mean value<sup>3</sup> of ( $\nu-\nu_0$ ) for the vibrationally purest  $\nu M-O$  band in the tris (tropolonato)  $[MT_3]$  complexes of the 3d-transition metal(III) ions. This approximates very reasonably with the difference in magnitude of the crystal field effects suggested by the thermodynamic data when we take account of the fact that the variation in  $\nu Ln-O$  will be reduced by vibrational coupling relative to a hypothetical vibrationally pure  $\nu Ln-O$  band.

## The alkaloid of *Propylaea quatuordecimpunctata* L. (Coleoptera, Coccinellidae)\*

**Summary:** The structure of a new alkaloid propylein, from the beetle *Propylaea quatuordecimpunctata* L., is shown to be II.

During our continuing study<sup>1,2</sup> of the defensive alkaloids of Coccinellidae we have examined the species *Propylaea quatuordecimpunctata* L. 800 specimens collected around Brussels during the summer of 1971 were blended in methanol, the supernatant was evaporated to dryness and reextracted with methylene chloride. Extraction of this solution with 5% HCl, followed by treatment with  $NH_4OH$  and another extraction with methylene chloride afforded about 20 mg of a new compound, propylein that appears to be the sole alkaloid of the beetle.

Propylein has the empirical formula  $C_{13}H_{21}N$  (by mass spectrometry), was amorphous in our hands and is laevorotatory. The compound undergoes rapid degradation when kept as the free base. Its NMR spectrum shows an absorption of 3H at 0.92 ppm (ill-resolved doublet:  $CH_3-CH$ ), a broad absorption of 2H from 3.05 to 3.20 ppm ( $HC-N$ ) and one multiplet of 1H at 4.78 ppm ( $HC=C$ ). The frequency of the olefinic proton is in agreement with values reported for enamine systems of the type  $N-C=CH^3$ . The presence of such a grouping is also indicated by a band at  $1668\text{ cm}^{-1}$  in the IR spectrum. Propylein, however, has only end-absorption in the UV.

The fragmentation pattern observed in the mass spectrum of propylein very closely parallels that of precoccinellin<sup>2</sup>, the tertiary amine corresponding the coccinellin (I), with all peaks shifted downwards by two mass units. This suggested a close relationship of structures and led to the hypothesis that propylein is one of the three possible dehydroprecoccinellins possessing only one olefinic proton. This was established by hydrogenation

### Experimental

The lithium salts of the complex anions were prepared by the reported<sup>5</sup> procedures. Infrared spectra were determined on a Beckman IR-12 spectrophotometer on Nujol mulls between caesium bromide plates. The frequency of the band assigned to  $\nu Ln-O$  was determined five times for each complex. Maximum discrepancy in this frequency was  $0.5\text{ cm}^{-1}$ . For maximum precision, frequencies were read from the wavenumber drum, not the chart paper.

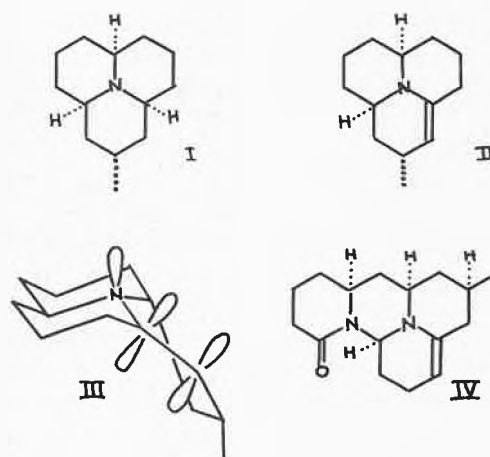
### Acknowledgements

We thank Professor G. ANDEREGG for helpful discussion on stability relationships in lanthanide complexes and for hospitality extended to one of us (D.A.T.) while on study leave during 1971 at the Laboratorium für anorganische Chemie der Eidgenössischen Technischen Hochschule Zürich. We thank the University of Cape Town Research Grants Committee and the South African Council for Scientific and Industrial Research for financial assistance.

L. G. HULETT and D. A. THORNTON

Department of Physiology and Medical Biochemistry and  
Department of Chemistry  
University of Cape Town (South Africa)

of propylein over platinum oxide, yielding a compound identical with precoccinellin ( $R_f$  on TLC, MS). The reaction product was further oxidized with monopero-phthalic acid to afford coccinellin (I), identical in all respects with an authentic sample.



Since the proposed structure I of coccinellin has been confirmed by X-ray diffraction<sup>4</sup>, one can deduce the structure II of propylein. Of the three possible dehydro-

\* Received Dezember 15, 1971.

<sup>1</sup> B. TURSCH, D. DALOZE, M. DUPONT, J. M. PASTEELS and M. C. TRICOT, *Experientia*, in press.

<sup>2</sup> B. TURSCH, D. DALOZE, M. DUPONT, C. HOOTELE, M. KAISIN, J. M. PASTEELS and D. ZIMMERMANN, *Chimia* 25 (1971) 307.

<sup>3</sup> W. A. AYER, J. K. JENKINS, S. VALVERDE-LOPEZ and R. H. BURNELL, *Can. J. Chem.* 45 (1967) 433.

<sup>4</sup> D. LOSMAN and R. G. KARLSSON, personal communication (to be published shortly).

precocinellins mentioned above, only one can be expected to be devoid of the UV absorption typical of enamines. Indeed, as shown in figure III, the  $\pi$ -electrons system of the double bond and the unshared electrons of the nitrogen atom cannot be parallel in structure II. A very similar situation is found in the alkaloid anhydrolycococerin (IV)<sup>5</sup>, which also shows only end-absorption in the

UV. The structure presented here for propylein has no implication regarding its absolute configuration.

B. TURSCH, D. DALOZE and C. HOOTELE  
Université Libre de Bruxelles, Brussels (Belgium)

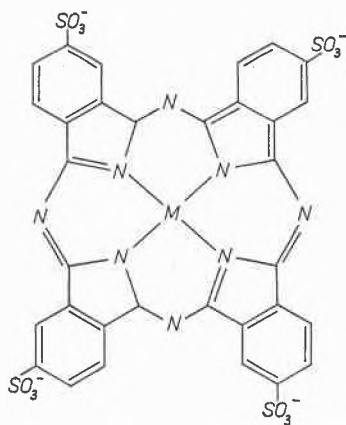
<sup>5</sup> N. MILLER, C. HOOTELE, C. BRAEKMAN-DANHEUX and J. C. BRAEKMAN, *Bull. Soc. Chim. Belg.*, in press.

## Reversible Reaction of Cobalt(II) Tetrasulfophthalocyanine with Molecular Oxygen\*

### Summary

Absorption spectra of solutions of Co (II), Fe (III) and Mn (III) tetrasulfophthalocyanines have been studied under aerobic and anaerobic conditions. CoTSP reacts reversibly with molecular oxygen forming a stable oxygen adduct. The oxygen adduct with FeTSP is stable only in neutral solution and its formation is not fully reversible. No reaction of MnTSP with oxygen has been found.

During the study of catalytic effects of cobalt(II) tetrasulfophthalocyanine (CoTSP, formula I) on autoxidation reactions marked changes of absorption spectra of CoTSP solutions with time were found<sup>1</sup>. Various effects of experimental conditions on absorption spectra of metal tetrasulfophthalocyanines were formerly described by some other authors<sup>2-5</sup>. BERNAUER and FALLAB<sup>2</sup> found that absorption spectra of CoTSP in aqueous and non-aqueous solutions are significantly different. The authors ascribed these differences to the existence of monomeric and dimeric forms of CoTSP in solution and to the respective shifts of the equilibrium position. This conception of equilibrium between monomeric and dimeric forms was also used by KOBAYASHI *et al.*<sup>3</sup>, and later by AHRENS and KUHN<sup>4</sup> for the explanation of the influence of surface active substances and of concentration changes. None of all these authors, however, report a time change of absorption spectrum.



In our experiments the changes of absorption spectra of CoTSP solutions in nitrogen and in oxygen atmosphere

were followed. The absorption spectrum of freshly prepared alkaline solution of CoTSP shows two absorption bands, at 626 and 670 nm (Fig. 1, curve 1). In the presence of oxygen the absorption at 626 nm gradually decreases and that at 670 nm increases at the same time (Fig. 1, curve 2). The limiting values are reached within several hours or days, according to temperature and to pH. If the oxygenated solution of CoTSP is being bubbled with thoroughly purified oxygen-free nitrogen at 70°C the reverse reaction occurs (Fig. 1, curve 3, 4). The bubbling with nitrogen at room temperature is without any effect. The whole cycle consisting of oxygenation and deoxygenation can be repeated many times without any noticeable irreversible change. The occurrence of the isosbestic point at 645 nm (Fig. 1) demonstrates the presence of only two absorbing substances in the solution and the reversibility of the transformation described.

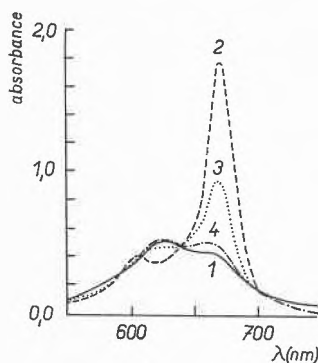


Fig. 1. Absorption spectrum of CoTSP

Curve 1 fresh solution  
Curve 2 after 150 min bubbling with O<sub>2</sub>  
Curve 3 after 60 min bubbling with N<sub>2</sub> at 70°C  
Curve 4 after 120 min bubbling with N<sub>2</sub> at 70°C  
1 · 10<sup>-5</sup> M CoTSP; 0,1 M NaOH

\* Received Dezember 16, 1971.

<sup>1</sup> D. M. WAGNEROVÁ, E. SCHWERTNEROVÁ and J. VEPŘEK-ŠIŠKA, *Coll. Czech. Chem. Commun.*, in press.

<sup>2</sup> K. BERNAUER and S. FALLAB, *Helv. Chim. Acta* 44 (1965) 1287.

<sup>3</sup> H. KOBAYASHI, Y. TORII and N. FUKADA, *J. Chem. Soc. Japan* 81 (1960) 694.

<sup>4</sup> U. AHRENS and H. KUHN, *Z. physik. Chem. (Frankfurt)* 37 (1963) 1.

<sup>5</sup> J. H. WEBER and D. H. BUSCH, *Inorg. Chem.* 4 (1965) 472.

Reversible oxygenation of CoTSP can be proved also in acid solution. When compared with the alkaline solution the difference is that the oxygenated form of CoTSP is less stable and can be decomposed by bubbling with nitrogen even at room temperature within several minutes. Irreversible changes of absorption spectra, caused probably by the decomposition of CoTSP, can be noticed already after one hour.

From the results presented it is evident that the absorption band at 626 nm belongs to the CoTSP, the absorption band at 670 nm to an adduct of CoTSP with molecular oxygen. These absorption bands can by no means be ascribed to the existence of monomeric and dimeric species in solution. The properties of the oxygen adduct resemble closely those of the well described synthetic reversible oxygen-carrying chelates<sup>6</sup>. It may be assumed that the composition of the CoTSP adduct is similar to the other oxygen-carriers represented either by the formula  $\text{CoTSP} \cdot \text{O}_2$  or  $\text{CoTSP} \cdot \text{O}_2 \cdot \text{CoTSP}$ .

Experiments, similar to those previously mentioned, have been made with Mn(III) and Fe(III) tetrasulphophthalocyanines. In alkaline solution MnTSP shows a sharp band at 684 nm and a lower one at 626 nm. The complicated change of the absorption spectra with time can be explained, in agreement with FENKART and BRUBAKER<sup>7</sup>, as the result of hydrolytic processes. No effect of oxygen was found.

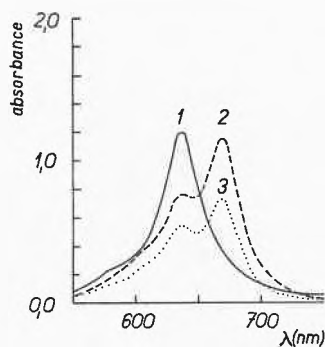


Fig. 2. Absorption spectrum of FeTSP

Curve 1 fresh solution

Curve 2 after 10 min bubbling  $\text{N}_2$  at  $70^\circ\text{C}$

Curve 3 after 10 min bubbling  $\text{O}_2$  at  $70^\circ\text{C}$

$2 \cdot 10^{-5}$  M FeTSP; 0,1 M NaOH

The absorption spectrum of the fresh alkaline solution of Fe(III)TSP (formulated according to WEBER and BUSCH<sup>8</sup>) shows a sharp band at 634 nm, which decreases with time (Fig. 2, curve 1). Simultaneously a new band at 668 nm appears and reaches its limit within 6 hours at room temperature. Subsequently a slow decomposition of the complex is observed. The increase of the band at

668 nm is independent on aerobic or anaerobic conditions and is entirely irreversible (Fig. 1, curve 2, 3). An opposite reaction, i.e. an increase of the original band at 634 nm, was never found.

The absorption spectrum of the FeTSP solution in water ( $\text{pH} = 6,5$ ) does not change with time. The bubbling of purified nitrogen through the solution at  $70^\circ\text{C}$  causes an increase of the band at 668 nm i.e. the same change as occurs during the ageing of the alkaline solution. This change, however, can be reversed by the action of oxygen. The reversible reaction is probably accompanied by partial breakdown of the complex, as the full initial height of the band could not be reached.

The behaviour of FeTSP in neutral solution is almost identical with that described by VONDERSCHMITT, BERNAUER and FALLAB<sup>9</sup> in spite of the fact that their initial product was Fe(II)TSP characterized by an absorption band at 670 nm. These authors found an increase of absorption at 623 nm under oxygen; the change can be reversed by the influence of nitrogen at  $70^\circ\text{C}$ . The absorption band at 632 nm is ascribed to a binuclear adduct with oxygen  $\text{TSPFe} \cdot \text{O}_2 \cdot \text{FeTSP}$ . Though it could be possible that compounds formulated as Fe(III)TSP and  $\text{TSPFe(II)} \cdot \text{O}_2 \cdot \text{Fe(II)TSP}$  had identical spectra (absorption band at 632 to 634 nm) it seems more probable that in fact only one compound exists.

#### Experimental

Metal tetrasulphophthalocyanines were prepared according to WEBER and BUSCH<sup>8</sup> by melting sodium salt of sulfophthalic acid, urea, ammonium chloride and respective metal chloride. The crude product was purified by repeated dissolving and salting out from the solution, washing with ethanol-water mixture and extracting by absolute ethanol.

Other chemicals were of analytical grade.

Absorption spectra were measured with a recording spectrophotometer Unicam SP 800 B, in cells of 1 cm path length. The cells were sealed by silicon rubber. The solution was bubbled with gas directly in the cuvette by means of an injection needle put through the rubber closure. Nitrogen was purified from traces of oxygen by bubbling through Cr(II) chloride solution.

J. VEPŘEK-ŠIŠKA, E. SCHWERTNEROVÁ  
and D. M. WAGNEROVÁ

Institute of Inorganic Chemistry  
Czechoslovak Academy of Sciences, Prague

<sup>6</sup> E. BAYER and P. SCHRETTZMANN, *Structure & Bonding* 2 (1967) 181.

<sup>7</sup> K. FENKART and C. H. BRUBAKER jr., *J. Inorg. Nucl. Chem.* 30 (1968) 3245.

<sup>8</sup> J. H. WEBER and D. H. BUSCH, *Inorg. Chem.* 4 (1965) 469.

<sup>9</sup> D. VONDERSCHMITT, K. BERNAUER and S. FALLAB, *Helv. Chim. Acta* 48 (1965) 951.

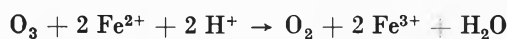
Oxydation de  $\text{Fe}^{2+}$  par  $\text{O}_3$  en réacteur semi-continu parfaitement agité\*

## Abstract

Ferrous ion oxidation by ozonised air was carried out in a laboratory well-mixed semi-flow batch reactor. Ozone transfer is shown to proceed according to ASTARITA's fast reaction regime. Experimental data are compared to figures obtained by means of the reactor model equation, the use of which is made very simple by introducing a dimensionless group ( $J$ ), which is directly related with the ozone reaction efficiency. A method is thereby established for the determination of the interfacial mass transfer area as a function of agitation and superficial gas velocity.

## 1. Introduction

Traitant l'oxydation irréversible



en présence d'un grand excès de  $\text{Fe}^{2+}$ , comme une réaction de pseudo-premier ordre, CONOCCHIOLI et coll.<sup>1</sup> ont déterminé à 25°C et en milieu perchlorique, une constante cinétique

$$k = (1,7 \pm 0,4) 10^5 \text{ M}^{-1} \text{ sec}^{-1}.$$

Nous réalisons cette oxydation en réacteur semi-continu parfaitement agité, en solution sulfurique de pH 2. Selon la classification que donne ASTARITA<sup>2</sup> des phénomènes d'absorption accompagnés de réaction chimique, le réacteur fonctionne en régime de «réaction rapide».

L'équation de fonctionnement du réacteur conduit à la définition d'un nombre adimensionnel ( $J$ ) qui décrit de façon frappante l'efficacité avec laquelle le réactif gazeux est consommé par la réaction en phase liquide.

## 2.1. Calcul d'un réacteur semi-continu parfaitement agité

Réalisons la réaction  $\text{A} + n\text{B} \rightarrow \text{produits}$ , dont la cinétique est du type  $r_A = kab$ , dans le réacteur représenté à la Fig. 1, et fixons les conditions de telle sorte que soit réalisé le régime de «réactions rapide» (voir 2.2).

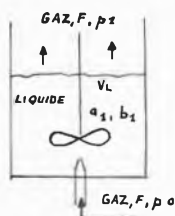


Fig. 1  
Réacteur semi-continu parfaitement agité

Supposons que  $p_0$ , pression de A à l'entrée, soit assez faible pour qu'on puisse négliger la variation du débit gazeux  $F$  entre l'entrée et la sortie.

Le bilan de A, relatif à la phase gazeuse, s'écrit :

$$(p_0 - p_1) \frac{F}{RT} - a_L V_L K_L (a_e - a_1) = 0 \quad (1)$$

avec  $a_e H = p_1$ .

$a_L$  : aire interfaciale par unité de volume de phase liquide. Dans la phase liquide, les bilans de A et B sont :

$$V_L \frac{da_1}{dt} - a_L V_L K_L (a_e - a_1) + k a_1 b_1 V_L = 0, \quad (2)$$

$$V_L \frac{db_1}{dt} + n k a_1 b_1 V_L = 0. \quad (3)$$

Avec les hypothèses suivantes :

- régime de réaction rapide:  $a_1 = 0$  dans (2),
- résistance en phase gazeuse négligeable, et réaction de pseudo-premier ordre :

$$K_L = k_L = \sqrt{k b_1 D} \quad (\text{voir 2.2}),$$

et en posant  $Z = b_1/b_0$ ,  $b_0$  étant la concentration de B au temps  $t = 0$ , on obtient par intégration :

$$2(1 - \sqrt{Z}) + \frac{V_L RT}{HF} M(1 - Z) = \frac{p_0}{b_0} \frac{n}{H} M t \quad (4)$$

avec

$$M = a_L \sqrt{k b_0 D}. \quad (5)$$

En faisant  $Z = 0$  dans (4), on obtient le temps nécessaire à la transformation complète du réactif B en phase liquide :

$$t_f = \left( \frac{M + 2HF/V_L RT}{M} \right) \frac{b_0 V_L}{n N}, \quad (6)$$

$N$  étant le débit molaire du réactif gazeux A.

Le temps  $\frac{b_0 V_L}{n N} = t_m$  est évidemment le temps *minimum* pour transformer la totalité de B; la relation (6), réécrite

$$t_f = J t_m \quad (7)$$

signifie donc que le taux d'utilisation de A est de 100% lorsque  $J \cong 1$ . Le fonctionnement du réacteur s'écarte d'autant plus de ce caractère idéal, que la valeur de  $J$  est plus élevée.

2.2. Choix du régime d'absorption<sup>2</sup>

L'absorption d'un gaz A participant en phase liquide à une réaction  $\text{A} + n\text{B}$ , se produit en régime de «réaction rapide» à condition que le nombre de HATTA,  $\gamma$ , ait une valeur suffisante :

$$\gamma = \sqrt{k_1 D} / k_L^0 \geq 4 \text{ pour une réaction du premier ordre}^3.$$

Dans ce cas, le coefficient de transfert prend la forme très simple, indépendante de  $k_L^0$  :

$$k = \sqrt{k_1 D} = \sqrt{k b_1 D}. \quad (8)$$

\* Reçu le 25 décembre 1971.

<sup>1</sup> T. J. CONOCCHIOLI, E. J. HAMILTON jr. et N. SUTIN, *J. Amer. Chem. Soc.* 83 (1965) 926.

<sup>2</sup> G. ASTARITA, *Mass Transfer with Chemical Reaction*, Elsevier, 1967.

<sup>3</sup> H. HIKITA et S. ASAI, *Kagaku Kogaku* 27 (1963) 823.

Toutefois,  $k_L^0$  doit être estimé en vue du calcul de  $\gamma$ . Dans notre cas, on trouve  $k_L^0 = 0,019$  cm/sec (voir en annexe, le calcul de  $k_L^0$  et ses limitations). En retenant  $k = 2 \cdot 10^5$  M<sup>-1</sup> sec<sup>-1</sup> pour ordre de grandeur de la constante cinétique, il vient

$$\gamma = 15.$$

On réalise donc le régime de réaction rapide, et il en est ainsi tant que  $b_1$  reste supérieur à environ 5 à 10% de la valeur initiale  $b_0$  ( $= 2 \cdot 10^{-2}$  M).

### 3. Etude expérimentale

#### 3.1. Appareillage – déroulement d'un essai

Le réacteur semi-continu (Fig.1), d'un diamètre de 11,8 cm, est pourvu d'un agitateur Quickfit ST1/1 (2 pales, largeur 7,2 cm), et alimenté en gaz par un orifice de 0,1 cm de diamètre. Le circuit de gaz comporte un compresseur d'air, différents appareils de purification, un ozoniseur et un débitmètre à capillaire.

Un essai comporte l'action, à 25 °C, d'un courant d'air ozonisé sur 500 ml d'une solution sulfurique de Fe<sup>2+</sup> ( $b_0 = 2 \cdot 10^{-2}$  M), pendant un temps déterminé, le débit gazeux et la vitesse d'agitation étant fixés. Le pH est maintenu à 2 pendant l'essai. A la fin de celui-ci, on dose  $b_1 = [\text{Fe}^{2+}]$  par le dichromate en présence de diphénylamine.

Deux dosages de la teneur en O<sub>3</sub> de l'air ozonisé sont effectués, immédiatement avant et après l'essai. La moyenne des deux résultats (l'écart maximum observé est de 2,5%) permet de calculer le débit  $N$  d'ozone. Le dosage est réalisé par absorption dans une solution de KI tamponnée à pH 7, et titrage de l'iode par Na<sub>2</sub>S<sub>2</sub>O<sub>3</sub> 0,1 N, après acidification par H<sub>2</sub>SO<sub>4</sub> dilué<sup>4</sup>.

#### 3.2. Effets de l'agitation et du débit gazeux

La Fig.2 représente les courbes  $Z = b_1/b_0$  observées en fonction de  $t/t_m$ , au cours de 6 groupes d'essais effectués avec un débit d'air ozonisé identique, et comme paramètre, la vitesse de rotation  $N_T$  de l'agitateur.

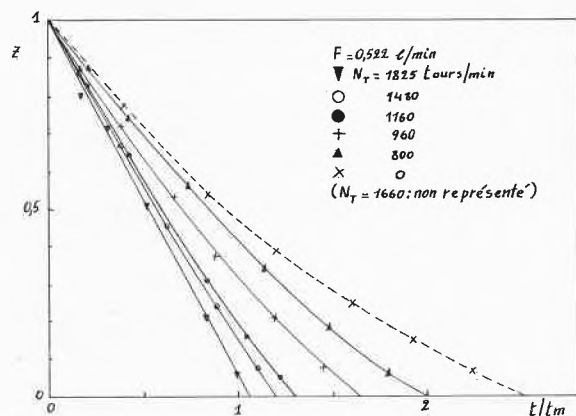


Fig. 2. Effet de l'agitation

Pour  $N_T = 1825$ , la décroissance de  $Z$  est linéaire, et le taux d'utilisation d'O<sub>3</sub> est voisin de 100%. A mesure que  $N_T$  décroît, le fonctionnement du réacteur se dégrade sensiblement, pour se rapprocher, à  $N_T = 800$ , de celui du réacteur non agité.

A la Fig.3, par contre, le paramètre variable est le débit  $F$ , tandis que  $N_T$  est constant. On voit que l'augmentation du débit gazeux entraîne une diminution progressive du taux d'utilisation de l'ozone.

### 4. Discussion et conclusion

Il découle de la relation (7) que, pour chaque groupe d'essais, le nombre  $J$  peut être relevé sur les graphiques des Fig.2 et 3;  $J$  n'est autre chose que l'abscisse de l'intersection de chacune des courbes avec l'axe  $Z = 0$ .

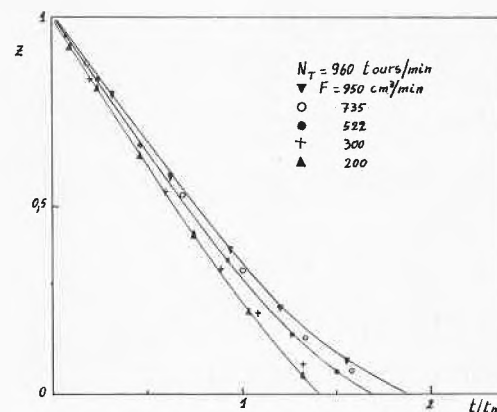


Fig. 3. Effet du débit gazeux

La connaissance de  $J$  permet alors le calcul de  $M$ , et finalement celui de  $a_L$  selon (5)\*. Les résultats sont rassemblés aux tableaux 1 et 2.

Tableau 1. Effet de l'agitation

$N_T$ (tours/min)	1825	1660	1480	1160	960	800
$J$	1,03	1,10	1,18	1,29	1,64	2,00
$M$ (sec <sup>-1</sup> )	4,65	1,41	0,78	0,48	0,22	0,14
$a_L$ (cm <sup>-1</sup> )	17	5,27	2,86	1,76	0,82	0,51

1° L'évolution du réacteur vers un fonctionnement idéal lorsque l'agitation croît est mise en évidence par les valeurs de  $J$ . A l'origine de cette évolution se trouve la forte dépendance de l'aire interfaciale  $a_L$  vis-à-vis de la vitesse d'agitation. La Fig.4 montre que dans le domaine de  $N_T$  étudié, la pente de la droite  $\log a_L / \log N_T$  a une valeur de 3.1.

Note: On a exclu de la Fig.4 le point ( $N_T = 1825$ ;  $a_L = 17$ ). Cette valeur élevée de  $a_L$ , physiquement peu significative, découle du fait que  $J$  est proche de 1. Par définition, en effet,  $a_L \rightarrow \infty$  lorsque  $J = 1$ . Puisqu'en pratique,  $a_L$  ne peut pas croître à l'infini, il est clair que  $J$  peu tout au plus tendre asymptotiquement vers 1.

2° Le débit gazeux est transformé au tableau 2 en «vitesse superficielle»  $V_S$ , i.e. débit rapporté à la section du réacteur. Lorsque  $F$  augmente, la détérioration

\* Nous prenons  $D = 2 \cdot 10^{-5}$  cm sec<sup>-1</sup> et  $H = 98$  atm litre mole<sup>-1</sup>.

progressive du fonctionnement du réacteur, observée expérimentalement, s'explique par l'accroissement parallèle de  $J$ . Celui-ci est dû au fait que  $M$  (proportionnel à  $a_L$ ) croît moins que proportionnellement à  $F$ . C'est du reste ce qu'on peut lire à la Fig. 4, ou la pente de la droite  $\log a_L / \log V_S$  est égale à 0,51.

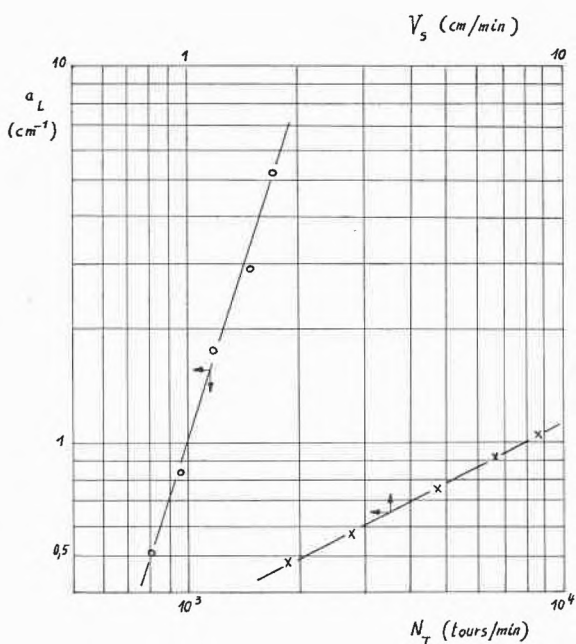


Fig. 4. Influence de l'agitation (O) et du débit gazeux (x) sur l'aire interfaciale

Tableau 2. Effet du débit gazeux

$F$ (cm <sup>3</sup> /min)	200	300	522	735	950
$V_S$ (cm/min)	1,82	2,73	4,75	6,67	8,63
$J$ -	1,40	1,51	1,69	1,79	1,89
$M$ (sec <sup>-1</sup> )	0,13	0,16	0,20	0,25	0,29
$a_L$ (cm <sup>-1</sup> )	0,48	0,57	0,74	0,91	1,04

### Conclusion

En régime de « réaction rapide », le coefficient de transfert d'absorption accompagnée de réaction chimique ne dépend pas du coefficient d'absorption physique  $k_L^0$ , mais essentiellement de l'aire interfaciale  $a_L$ . Nous avons illustré l'effet de cette variable-clé dans le cas de l'oxydation des ions ferreux par l'air ozonisé, en mettant en évidence l'effet sur  $a_L$  des variables opératoires agitation et débit gazeux. Le modèle proposé pour le fonctionnement du réacteur semi-continu parfaitement agité rend compte correctement des phénomènes expérimentaux.

### Annexe: Calcul de $k_L^0$

1. Calcul du diamètre des bulles gazeuses, émises par un orifice unique?

- à faible débit:  $d_b^0 = 6 D_0 \sigma / g(\rho_L - \rho_G)$   $d_b = 0,35$  cm
- à débit «intermédiaire»:  $d_b = 0,18 D_0^{0,5} N_{Re}^{0,33}$   $d_b = 0,35$  à  $0,6$  cm

Le premier des deux résultats est plus conforme à la réalité de nos essais. Mais la valeur choisie pour  $d_b$  n'influence pas le calcul de  $k_L^0$ , ainsi que l'indique le calcul effectué au moyen de la corrélation ci-dessous, et comme l'a montré CALDERBANK<sup>8</sup>.

2. Evaluation de  $k_L^0$ : pratiquement indépendant de l'agitation<sup>9</sup>,  $k_L^0$  est donné par la corrélation de HUGMARK relative aux systèmes à bulles isolées<sup>10</sup>:

$$N_{Sh} = \frac{k_L^0 d_b}{D} = 2 + 0,061 \left[ N_{Re}^{0,484} N_{Sc}^{0,338} \left( \frac{d_b \sigma^{1/3}}{D^{2/3}} \right)^{0,072} \right]^{1,01}$$

$$k_L^0 = 0,019 \text{ cm/sec.}$$

Si on admet l'existence d'interactions entre bulles, le facteur 0,061 est remplacé par 0,0187, et on obtient  $k_L^0 = 0,0058$  cm/sec. Cela conduit à  $\gamma \cong 45$  (voir 2.22), ce qui renforce l'hypothèse d'une « réaction rapide », sans que ne soit atteint le régime de « réaction instantanée ».

### Notations

$a, b$	concentrations de A, B, respectivement réactif gazeux et liquide	mole/litre
$a_L$	aire interfaciale par unité de volume de phase liquide	cm <sup>-1</sup>
$d_b$	diamètre des bulles gazeuses	cm
$D$	diffusivité de A dans la phase liquide	cm <sup>2</sup> /sec
$D_0$	diamètre de l'orifice d'alimentation de gaz	cm
$F$	débit gazeux	cm <sup>3</sup> /min
$H$	constante de HENRY	litre atm/mole
$J$	$(M + 2 HF / V_L RT) / M$	-
$k_1$	constante cinétique de pseudo-premier ordre	sec <sup>-1</sup>
$k_L, K_L$	coefficient de transfert en phase liquide, avec réaction chimique	cm/sec
$k_L^0$	coefficient de transfert en phase liquide, sans réaction chimique	cm/sec
$M$	$a_L \sqrt{k b_0 D}$	sec <sup>-1</sup>
$n$	coefficient stœchiométrique	-
$N$	débit molaire de A	mole/sec
$N_T$	vitesse de rotation de l'agitateur	tours/min
$p$	pression partielle de A	atm
$t_f$	temps d'épuisement du réactif B	min
$t_m$	temps minimum d'épuisement du réactif B	min
$V_L$	volume de phase liquide	litre
$V_S$	vitesse superficielle de la phase gazeuse	cm/min
$Z$	$b_1/b_0$ , proportion de réactif B substituant au temps $t$	-
$\gamma$	nombre de HATTA, $\sqrt{k_1 D} / k_L^0$	-
$\sigma$	tension interfaciale gaz-liquide	g/cm
$g \rho_L, g \rho_G$	poils spécifiques, phases liquide et gazeuse	g/cm <sup>3</sup>

ANDRÉ SCHREIBER

Université Nationale du Zaïre, Campus de Lubumbashi, B.P. 1825, Lubumbashi (République du Zaïre)

<sup>4</sup> Methoden der organischen Chemie (HUBEN-WEYL) VII/1 (1954) 338, G. THIEME.

<sup>5</sup> PERRY, Chemistry and Engineering, Handbook, 4<sup>e</sup> édition, 1963, p. 14.

<sup>6</sup> KIRK-OTHMER, Encyclopedia of Chemical Technology 9 (1952) 736.

<sup>7</sup> R. W. SCHAFTLEIN et T. W. F. RUSSEL, Ind. Eng. Chem. 60 (1968) 5, 12.

<sup>8</sup> P. H. CALDERBANK et M. B. MOO-YOUNG, Chem. Eng. Sci. 16 (1961) 39.

<sup>9</sup> S. SIDEMAN, O. HORTACSU et J. W. FULTON, Ind. Eng. Chem. 58 (1966) 7, 32.

<sup>10</sup> G. A. HUGMARK, Ind. Eng. Chem. Process Design Develop. 6 (1967) 2, 218.